

01 Nov 2006

## On One-dimensional Self-assembly of Surfactant-coated Nanoparticles

Jee-Ching Wang

Missouri University of Science and Technology, [jcwang@mst.edu](mailto:jcwang@mst.edu)

Partho Neogi

Missouri University of Science and Technology, [neogi@mst.edu](mailto:neogi@mst.edu)

Daniel Forciniti

Missouri University of Science and Technology, [forcinit@mst.edu](mailto:forcinit@mst.edu)

Follow this and additional works at: [https://scholarsmine.mst.edu/che\\_bioeng\\_facwork](https://scholarsmine.mst.edu/che_bioeng_facwork)

 Part of the [Chemical Engineering Commons](#)

---

### Recommended Citation

J. Wang et al., "On One-dimensional Self-assembly of Surfactant-coated Nanoparticles," *Journal of Chemical Physics*, American Institute of Physics (AIP), Nov 2006.

The definitive version is available at <https://doi.org/10.1063/1.2375091>

This Article - Journal is brought to you for free and open access by Scholars' Mine. It has been accepted for inclusion in Chemical and Biochemical Engineering Faculty Research & Creative Works by an authorized administrator of Scholars' Mine. This work is protected by U. S. Copyright Law. Unauthorized use including reproduction for redistribution requires the permission of the copyright holder. For more information, please contact [scholarsmine@mst.edu](mailto:scholarsmine@mst.edu).

# On one-dimensional self-assembly of surfactant-coated nanoparticles

Jee-Ching Wang,<sup>a)</sup> P. Neogi, and Daniel Forciniti*Department of Chemical and Biological Engineering, University of Missouri-Rolla, Rolla, Missouri 65409-1230*

(Received 27 July 2006; accepted 2 October 2006; published online 21 November 2006)

Nanometer-sized metal and semiconductor particles possess novel properties. To fully realize their potential, these nanoparticles need to be fabricated into ordered arrays or predesigned structures. A promising nanoparticle fabrication method is coupled surface passivation and self-assembly of surfactant-coated nanoparticles. Due to the empirical procedure and partially satisfactory results, this method still represents a major challenge to date and its refinement can benefit from fundamental understanding. Existing evidences suggest that the self-assembly of surfactant-coated nanoparticles is induced by surfactant-modified interparticle interactions and follows an intrinsic road map such that short one-dimensional (1D) chain arrays of nanoparticles occur first as a stable intermediate before further assembly takes place to form higher dimensional close-packed superlattices. Here we report a study employing fundamental analyses and Brownian dynamics simulations to elucidate the underlying pair interaction potential that drives the nanoparticle self-assembly via 1D arrays. We find that a pair potential which has a longer-ranged repulsion and reflects the effects of surfactant chain interdigitation on the dynamics is effective in producing and stabilizing nanoparticle chain arrays. The resultant potential energy surface is isotropic for dispersed nanoparticles but becomes anisotropic to favor the growth of linear chain arrays when self-assembly starts. © 2006 American Institute of Physics. [DOI: 10.1063/1.2375091]

## INTRODUCTION

Inorganic nanoparticles possess unique chemical, optical, electric, and magnetic properties unavailable in either molecular or bulk limit<sup>1-6</sup> due to their large fractions of surface atoms and quantum-scale dimensions. Moreover, they can be utilized as building blocks,<sup>5-8</sup> much like atoms in a natural crystal, to enable a bottom-up approach. These nanoparticles have thus been recognized as an ideal foundation for developing next-generation technologies in a wide range of fields including catalysis, nanoelectronics, photodetector, chemical and biological sensors, etc.<sup>5-8</sup> To fully realize their potential, it is essential to fabricate nanoparticles into ordered arrays or predesigned structures in order to obtain predictable characteristics.

To prevent fractal aggregation even at higher concentrations during self-assembly,<sup>5,6,9-12</sup> several methods have been developed; among them is coating nanoparticles with surfactants where one end of the surfactant chain is strongly anchored to the surface usually covalently, and the other end is free. In contrast to their bare counterparts, these nanoparticles remain well dispersed/dissolved in relatively dilute solutions. At higher concentrations, they exhibit a strong propensity to self-assemble into ordered arrays when deposited on a smooth solid surface or at the water-air interface in a Langmuir trough.

The effective interactions between colloidal particles determine their stability and phase behavior. The fact that on applying the surfactant coat nanoparticles shift in their aggregation behavior from fractals to ordered self-assembly

can be understood in the form of changed interparticle potential due to the surface modification. Note that in nanoparticles, the surface effects are as important as the bulk effects. Surfactants of different types and lengths have thus been used as a means to further tune the interparticle interactions. Although the occurrence of self-assembly can be phenomenologically interpreted as an outcome of reduced/passivated interparticle attraction, it still needs a demonstration. The pair interaction potentials that drive nanoparticle self-assembly consist of repulsion and attraction components resulting from different molecular-scale characteristics of the nanoparticle systems. Detailed information could be obtained from first-principles methods.<sup>13,14</sup> However, the level of complexity and the insufficiency of relevant information make it very difficult for such methods to be immediately useful. We employ an alternative approach in this work by using the experimental findings to model critical features of the pair potential and then Brownian dynamics simulations are used to confirm our expectations. The main objective is to formulate an analytic coarse-grain pair potential that exhibits the effects of adsorbed surfactants and induces the nanoparticle self-assembly as observed in the experiments. For this purpose, we consider a particular type of nanoparticles that is commonly used to study self-assembly, namely, the charge-neutral nanoparticles of a nanocrystalline core that is modestly spherical and a dense shell of monofunctional surfactant uniformly coated on the particle surface. Gold thiol  $[\text{Au}_m(\text{S}-R)_n]$  is the best known example.

Existing experimental studies show that the self-assembly of the nanoparticles under consideration here follows a particular path during self-assembly on a solid surface or at the water-air interface. Short one-dimensional (1D)

<sup>a)</sup>Electronic mail: jcwang@umr.edu

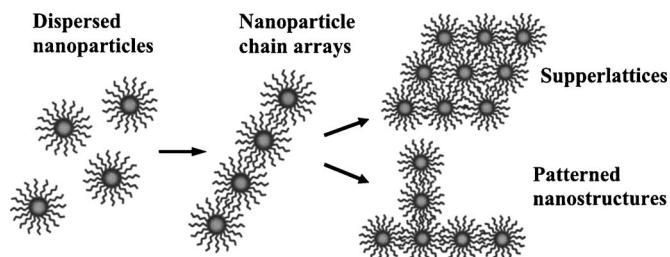


FIG. 1. Schematics of surfactant-coated nanoparticles and different self-assembly products. The Hamaker constant  $A_{11}=22.92 \times 10^{-19}$  J is somewhat smaller than Au–Au as suggested by the experiments. For the Morse potential  $\epsilon/\epsilon_{\text{Au–Au}}=36.216$ ,  $2R_g\beta=9.044$  and for Lennard-Jones  $\epsilon/\epsilon_{\text{Au–Au}}=36.216$  and  $\sigma/2R_g=1.095$ .

chain arrays of nanoparticles occur first as stable intermediate products,<sup>11,12</sup> as shown schematically in Fig. 1. Then the nanoparticle chain arrays further aggregate to form higher dimensional close-packed superlattices. Additional roles of nanoparticle chain arrays have also been envisioned in a number of emerging technologies.<sup>5,6</sup> It is very important to point out that with a generic spherical shape, zero electric charge, and uniform surfactant coating, the surfactant-coated nanoparticles should be *isotropic* without directional preference in their interactions when individually dispersed. Nevertheless, they self-assemble into *anisotropic* chain arrays instead of isotropic close-packed clusters. “Patchy” or directional potentials have been purposely formulated in simulation studies to produce similar particle chains.<sup>15,16</sup> While these potentials may be appropriate for chainlike aggregates of particles having rod shapes,<sup>17</sup> inhomogeneous surfactant coating,<sup>18</sup> or opposite charges,<sup>19,20</sup> and of electrorheological<sup>21</sup> (ER) and magnetorheological<sup>22</sup> (MR) particles under an electric or magnetic fields, they do not comply with the isotropic nature of dispersed surfactant-coated nanoparticles or represent a model suitable for producing and studying two-dimensional (2D) and three-dimensional (3D) assemblies. A criterion we followed in establishing a legitimate coarse-grain pair potential for the surfactant-coated nanoparticles is that the self-assembly is guided not by any purpose-built anisotropic interaction but rather by a unique combination of general isotropic interactions. The knowledge and understanding achieved in this study are believed to be of importance and value to the processing of colloidal systems in general and nanoparticle self-assembly in particular.

## MODEL POTENTIAL

Our attempt to establish a coarse-grain potential model for surfactant-coated nanoparticle proceeds in steps. Short-range (primary) repulsion and van der Waals (vdW) attraction are the first to be included in the nanoparticle pair potential, but for the bare particles. The former characterizes the excluded volume and is usually expressed as a steep exponential function. The latter causes nanoparticles to assemble and is typically described by a Hamaker potential in colloidal studies:<sup>23</sup>

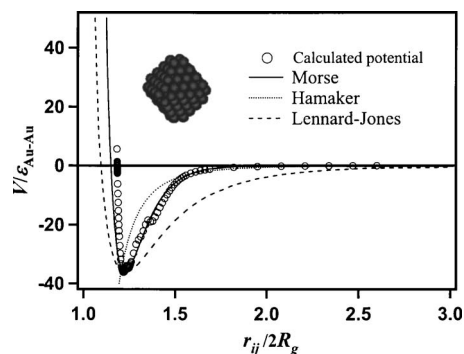


FIG. 2. Reduced pair interaction potential between the model  $\text{Au}_{140}$  nanoparticles as a function of reduced center-of-mass separation.  $R_g$  is the nanoparticle radius of gyration. The Hamaker constant  $A_{11}=22.92 \times 10^{-19}$  J is somewhat smaller than Au–Au as suggested by the experiments. For the Morse potential  $\epsilon/\epsilon_{\text{Au–Au}}=36.216$ ,  $2R_g\beta=9.044$  and for Lennard-Jones  $\epsilon/\epsilon_{\text{Au–Au}}=36.216$  and  $\sigma/2R_g=1.095$ .

$$\frac{E_{\text{Hamaker}}}{\epsilon_{\text{Au–Au}}} = -\frac{1}{12} \left( \frac{A_{11}}{\epsilon_{\text{Au–Au}}} \right) \left\{ \frac{1}{(r_{ij}/2R_g)^2 - 1} + \frac{1}{(r_{ij}/2R_g)^2} + 2 \ln \left[ \frac{(r_{ij}/2R_g)^2 - 1}{(r_{ij}/2R_g)^2} \right] \right\}, \quad (1)$$

where  $A_{11}$  is the Hamaker constant,  $r_{ij}$  is the center-to-center distance, and  $R_g$  is the radius of gyration. Some models for coated colloidal particles appear to be very appropriate for use here.<sup>24</sup> The key shortcomings of Hamaker interaction are that the primary minimum is infinitely deep and it is a continuum model that does not take into account the lattice spacing which can be inappropriate for the nanoparticles. To probe this issue, we used model bare nanoparticles that have 140 atoms in a face-centered-cubic (fcc) structure and a truncated octahedron shape (cf. Fig. 2). The interatomic interaction is described by a Lennard-Jones (LJ) potential whose parameters match the cohesive energy and lattice constant of Au. We varied and controlled the center-of-mass separation ( $r$ ) between two model Au nanoparticles while carrying out 3D rotation to compute the potential energy profile. The results in a dimensionless form are plotted in Fig. 2, together with the fitted curves. As indicated in Fig. 2, the Hamaker potential based on the nanoparticle radius of gyration and Au Hamaker constant tends to underestimate the nanoparticle vdW interaction, which can be attributed to the extreme smallness of the nanoparticles as discussed above. The LJ potential model is too soft, while the Morse potential model provides the most reasonable fit among the three:

$$\frac{E_{\text{Morse}}}{\epsilon_{\text{Au–Au}}} = \left( \frac{\epsilon}{\epsilon_{\text{Au–Au}}} \right) \left\{ [1 - e^{-(2R_g\beta)(r_{ij}/2R_g - r_{\text{min}}/2R_g)}]^2 - 1 \right\}, \quad (2)$$

$$\frac{E_{\text{LJ}}}{\epsilon_{\text{Au–Au}}} = 4 \left( \frac{\epsilon}{\epsilon_{\text{Au–Au}}} \right) \left[ \left( \frac{\sigma/2R_g}{r/2R_g} \right)^{12} - \left( \frac{\sigma/2R_g}{r/2R_g} \right)^6 \right]. \quad (3)$$

Consequently, Morse potential is used. A similar approach has been taken by Qin and Fichthorn.<sup>26</sup> In passing, we note that the effect of an intervening continuum dielectric/solvent modifies the energy parameters. We do not use the parameters employed in Fig. 2 for the later simulations and instead

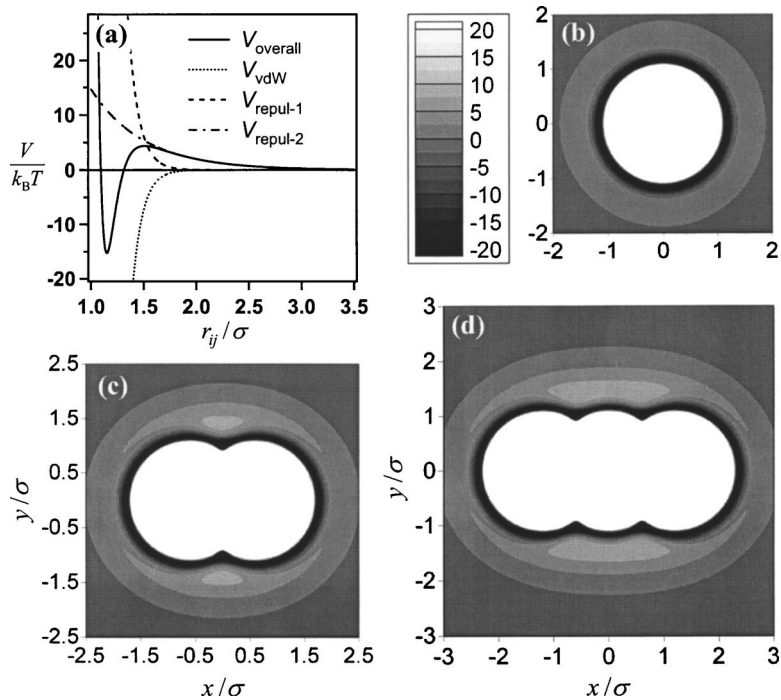


FIG. 3. Pair potential and resultant potential energy surfaces (PES). (a) A representative pair potential  $V/k_B T$  formulated for individual surfactant-coated nanoparticles.  $V_{\text{repul-1}}$  and  $V_{\text{repul-2}}$  are primary and secondary repulsions, respectively. (b) Contour plot of the PES experienced by a nanoparticle around a monomer, (c) around a dimer, and (d) around a trimer.

choose only the functional form of the potential based on the earlier discussion.

de Gennes studied the force due to the overlap of high coverage polymer chains end grafted on a solid surface and found it to be repulsive with exponential decay.<sup>23,25</sup> Repulsive force was also found between two surfaces with overlapping molecular-scale protrusions, which has also been described by an exponential function. Prompted by these findings, we included a longer-range (secondary), exponential repulsion to represent the effects of surfactant in the nanoparticle pair potential. As a result,

$$V(r) = \epsilon_{\text{rep-1}} e^{-\alpha_{\text{rep-1}}(r-\gamma_{\text{rep-1}})} + \epsilon_{\text{vdW}} \{ [1 - e^{-\beta(r-\gamma_{\text{vdW}})}]^2 - 1 \} + \epsilon_{\text{rep-2}} e^{-\alpha_{\text{rep-2}}(r-\gamma_{\text{rep-2}})}, \quad (4)$$

Thus, from left to right in Eq. (1), we have short-range repulsion due to chains and the Morse potential and the long-range repulsion due to the chains.

A second type of consideration enters at this point. It is well known that the presence of a layer around a colloidal particle (here the alkyl chains) attenuates the long-range attraction.<sup>24</sup> However, these chains being polymeric bring about a steric effect which produces a yet longer range repulsion<sup>23</sup> that would mask the shortcomings in the attractive forces. The net requirement is that with increasing separations, the primary minimum be followed by a secondary maximum/repulsion which is softer and longer ranged. It leads to  $\epsilon_{\text{rep-1}} > \epsilon_{\text{rep-2}}$ ,  $\alpha_{\text{rep-1}} > \alpha_{\text{rep-2}}$ , and  $\gamma_{\text{rep-1}} < \gamma_{\text{rep-2}}$  as a feasible option. Another requirement is that the secondary maximum should occur where chains overlap. By adjusting the relative values of the parameters, the pair potential of interest here was found as shown in Fig. 3(a) and the potential parameters in reduced units are listed in Table I. The secondary repulsion there dominates the pair potential at larger separations but yields to a stronger vdW attraction at smaller separations to result in a peaked repulsion preceding

a deep attraction energy well. Based on this pair potential, the 2D contour plot of the potential energy surface (PES) experienced by a nanoparticle approaching another monomeric nanoparticle is shown in Fig. 3(b), which is clearly isotropic and indicates that the second nanoparticle can attach from any angle to form a dimer as long as it has sufficient energy to overcome the repulsion barrier. However, when a nanoparticle approaches a dimer, the combination of two sets of isotropic pair potential, or more specifically two secondary repulsions, from the dimer creates an anisotropic PES shown in Fig. 3(c) that offers conical spaces of less resistance to nanoparticle attachment at the two ends. The formation of a linear trimer is hence favored over a more compact (triangular) one. It is easy to perceive that longer oligomers that can be formed by attachment of single nanoparticles or by collision between smaller oligomers should have similar PES and growth scenario [cf. Fig. 3(d)]. Fichtorn *et al.*<sup>27</sup> have shown in two dimensions that the exist-

TABLE I. Reduced values of the parameters in the pair potential, Eq. (4), and in the model of sliding resistance, Eq. (5).

Interaction component	Potential parameter	Reduced value
Primary repulsion	$\epsilon_{\text{rep-1}}$	$475.00k_B T$
	$\alpha_{\text{rep-1}}$	$10.00\sigma^{-1}$
	$\gamma_{\text{rep-1}}$	$1.07\sigma$
Secondary repulsion	$\epsilon_{\text{rep-2}}$	$2.00k_B T$
	$\alpha_{\text{rep-2}}$	$2.00\sigma^{-1}$
	$\gamma_{\text{rep-2}}$	$2.00\sigma$
van der Waals attraction	$\epsilon_{\text{vdW}}$	$621.37k_B T$
	$\beta$	$10.20\sigma^{-1}$
	$\gamma_{\text{vdW}}$	$1.00\sigma$
Sliding resistance	$r_{\text{inner}}$	$1.14\sigma$
	$r_{\text{outer}}$	$1.50\sigma$

tence of a secondary repulsion gives rise to ordered clusters of nanoparticles on a crystalline substrate. That is, the repulsion brings in a new set of constraints that are expected to play an important role. The present repulsion peaks around  $1.5\sigma$  and diminishes to nearly zero by  $3\sigma$ , and the resulting barriers in the PES at the sides and ends of longer arrays are very similar to those shown in Fig. 3(d), except covering longer distances at the two sides. The pair potential shown in Fig. 3(a) thus represents an effective, isotropic pair potential that has an actual ability to induce anisotropic self-assembly to form chain arrays.

Since this repulsion is important, we remark on its origins and magnitudes in more details below. The measured spacing between nanoparticles in an array reveals that surfactant chains on neighboring nanoparticles interdigitate.<sup>11,28,29</sup> This chain interdigitation results in a vdW attraction between surfactant-coated nanoparticles, or equivalently a deep energy valley in the PES that stabilizes the nanoparticle self-assembly. However, prior to the start of the chain interdigitation, solvent molecules confined between nanoparticles and having cohesive interaction with the surfactant chains need to be displaced out, and the dense layers of surfactant chains need to be opened up to accommodate each other. The former can be connected to a repulsive solvation force and the latter to a repulsive protrusion force.<sup>23</sup> Therefore, to achieve the observed chain interdigitation, work is required to overcome these repulsions and the required work can be translated into a repulsive energy barrier in the PES, which underlies the longer-range secondary repulsion discussed here. It can be further inferred that for surfactant-coated nanoparticles to exhibit desirable self-assembly, their secondary repulsion has a proper magnitude because otherwise nanoparticles would remain dispersed if it is too strong or experience hardly any energetic anisotropy if it is too weak. The first of these is known to be critical in stabilization of colloids using polymers.<sup>30</sup> The requirement of intermediate strength for the secondary repulsion could be associated with the fact that only a finite range of surfactant chain length enables the desired self-assembly.<sup>6,7,28</sup>

In principle, compact superlattices have lower energies than 1D chain arrays. That is, at this point of development in the pair potential, i.e., Eq. (1), 1D clusters would still prefer to eventually change into compact structures. For nanoparticle chain arrays to survive as feasible metastable products as observed in actual experiments, there must exist an intrinsic mechanism to provide an energy barrier against structure compactization driven by energy minimization. A valid mechanism for stabilizing intermediate 1D structure is provided by surfactant interdigitation because once nanoparticles self-assemble, the surfactant chains interdigitate and hinder significant angular displacement, i.e., sliding motion of one nanoparticle with respect to the other.

In experiments<sup>31,32</sup> with two polymer-coated plates under the condition of chain interdigitation/entanglement, sliding friction and sticking are encountered on moving one of the plates in the tangential direction [cf. Fig. 4(a)]. The former is dependent on the tangential velocity ( $v_{||}$ ) and is of dissipative nature, while the latter occurs at small separations and significant interdigitation. Brownian dynamics<sup>33</sup> is based

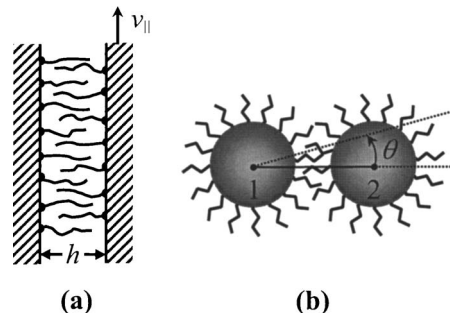


FIG. 4. Schematics of (a) polymer-coated plates in tangential motion and (b) surfactant-coated nanoparticles attempting sliding angular displacement.

on the decomposition of the total force in Langevin equation into these two parts to derive the Fokker-Planck equation. Equation (6) used here requires an added assumption that no changes take place in the time step  $\Delta t$ .<sup>33</sup> The velocity dependent force leads to the drag force and eventually into a Brownian diffusivity. This is either expressed in form of a function of a gap<sup>34</sup> or an overall effect such as in the use of Rotne-Prager-Yamaka tensor<sup>33</sup> which is an ensemble averaged diffusivity. We have not considered the complications in diffusivity because even our base case on diffusion in 2D is not properly characterized. Hence, only a constant diffusivity has been used. Use of this approximation disallows conservation of momentum, which in any case does not hold in Brownian dynamics because of the stochastic term to be encountered later in Eq. (6).

On the other hand, when the tangential velocity is suddenly set to zero or a plate is displaced tangentially under a sticking condition, a relaxation force will be felt on the moving plate to bring it back towards the original position by the interdigitated chains. The polymer-coated plates can thus experience tangential resistive forces under stationary conditions. These forces can be modeled as a potential such that there is a resistance felt to sliding. A simplified form of such a potential given below leads to zero force when the two particles move apart along the line of centers [cf. Fig. 4(b)].

In details, this new potential is

$$V_{\text{sliding}}(\theta, r_{ij}) = \begin{cases} \frac{1}{2}k_{\theta}\theta^2, & r_{ij} \leq r_{\text{inner}} \\ \frac{1}{2}k_{\theta}\theta^2 f(r_{ij}), & r_{\text{inner}} \leq r_{ij} \leq r_{\text{outer}} \\ 0, & r_{ij} \geq r_{\text{outer}}, \end{cases} \quad (5)$$

where, as shown in Fig. 4(b),  $\theta$  is the attempted angular displacement with respect to the line of centers between nanoparticles as they come to interdigitate with each other.  $V_{\text{sliding}}=0$  before chain interdigitation starts at  $r_{\text{outer}}$ , a separation slightly beyond the peaked repulsion, and  $V_{\text{sliding}} = \frac{1}{2}k_{\theta}\theta^2$  after maximum interdigitation has been reached at  $r_{\text{inner}}$ , a separation around the energy well [cf. Fig. 3(a) and Table I]. The sliding resistance should depend on the extent of chain interdigitation, and a cosine function,  $f(r_{ij}) = \frac{1}{2}[1 + \cos((r_{ij} - r_{\text{inner}})/(r_{\text{outer}} - r_{\text{inner}}))\pi]$ , was adopted in this work for convenient effectual handling of this dependence. The sliding resistance itself does not cause structural anisotropy simply because it can occur between any two interdigitated nanoparticles regardless of the assembled structure. As mentioned earlier, the harmonic component of sticking

counters lateral momentum or force, making the most probable trajectories taken by two particles when a dimer breaks down to be along their line of centers, which is what we expect. Conversely for flocculation, collisions at glancing angles are discouraged when one of the bodies is a dimer or a string because there the potential energy surface is already angle dependent as explained in Fig. 3.

## BROWNIAN SIMULATIONS

For the purpose of verifying the effectiveness of the formulated pair potential, Brownian dynamics simulations were carried out with the pair potential shown in Fig. 3(a) and a second-order algorithm,<sup>35</sup>

$$\Delta \mathbf{r}_{\text{pred}} = \frac{D}{k_B T} \mathbf{F}(\mathbf{r}) \Delta t + \Delta \mathbf{r}^R, \quad (6a)$$

$$\Delta \mathbf{r} = \frac{1}{2} \left[ \frac{D}{k_B T} \mathbf{F}(\mathbf{r}) + \frac{D}{k_B T} \mathbf{F}(\mathbf{r} + \Delta \mathbf{r}_{\text{pred}}) \right] \Delta t + \Delta \mathbf{r}^R, \quad (6b)$$

where  $D$  is the diffusivity of individual nanoparticles,  $k_B$  is Boltzmann's constant, and  $T$  is the absolute temperature.  $\mathbf{F} = -\nabla_{\mathbf{r}} V$  is the sum of pair interaction forces and thus depends on the locations of all nanoparticles.  $\Delta \mathbf{r}^R$  represents the stochastic displacement due to constant random collisions from solvent and is treated by a standard approach where  $\langle \Delta \mathbf{r}^R \Delta \mathbf{r}^R \rangle = 2D \Delta t \delta_{ij}$  and  $\delta_{ij}$  is the Kronecker delta. The trajectories were produced by first generating predicted locations according to Eq. (6a) for all nanoparticles based on current locations and then calculating the forces at the predicted locations to obtain the "corrected" displacements following Eq. (6b) over  $\Delta t$ . This algorithm resembles the predictor-corrector integration algorithm to better accommodate the relatively narrow energy well of the pair potential [cf. Fig. 3(a)] that could cause sudden strong repulsion to break apart the assembled nanoparticles. As usual, the Brownian dynamics simulations were carried out after non-dimensionalization with all the parameters and variables scaled by three base quantities, namely,  $\sigma$ ,  $k_B T$ , and  $D$ . The simulation time step adopted was  $\Delta t = 0.56 \times 10^{-6} \sigma^2 / D$ . The anisotropy of the pair potential significantly lowered the rates of successful collisions and self-assembly. Therefore, only lateral displacements (2D) were integrated for the sake of better efficiency, which should be as useful as 3D systems in verifying the pair potential.

Simulation was performed with 16 nanoparticles with the initial condition in form of a square lattice with an interparticle spacing of  $3\sigma$ , but interacting via the pair potential without the secondary repulsion and sliding resistance. Without these two surfactant-based interaction components, vdW attraction quickly drives nanoparticles to form dimers and then a close-packed hexagonal cluster within  $10^7 \Delta t$ 's. That is, compact clusters are formed. Alternatively, a linear array of nanoparticles separated by their equilibrium distance was used as an initial condition. The chain very quickly restructures to form compact clusters. Adding the secondary repulsion does not change these outcomes. In fact, too much of the secondary repulsion delays flocculation as expected.

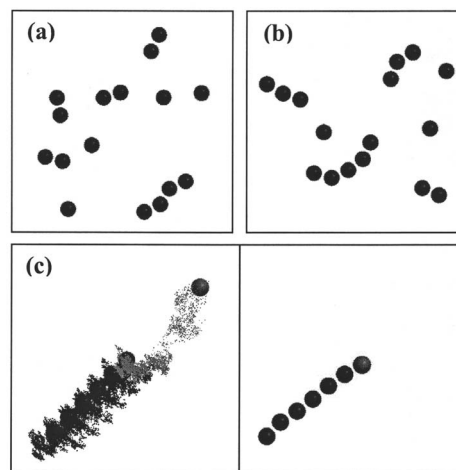


FIG. 5. Simulation snapshots. (a) With secondary repulsion and sliding resistance ( $k_\theta = 60k_B T$ ) after  $8 \times 10^7 \Delta t$ 's. (b) With secondary repulsion but without sliding resistance ( $k_\theta = 0$ ) after  $8 \times 10^7 \Delta t$ 's. (c) Initial (left panel) and final (right panel) configurations of a nanoparticle chain array superimposed with trajectories (dots) spanning  $4 \times 10^7 \Delta t$ 's.

Adding only the sliding resistance to the pair potential also does not alter the eventual outcome of the square-latticed nanoparticles significantly; a weak resistance only causes the nanoparticles to take a longer time to achieve close packing, while a strong resistance (e.g.,  $k_\theta = 200k_B T$ ) can provide a sufficient barrier to generate a hole or other defects in the final cluster. On the other hand, a strong sticking was found capable of maintaining the structure of nanoparticles with the initial configuration of a linear chain. Adding a secondary repulsion that is neither too small nor too large, to the sliding friction that forms the complete pair potential considered in this work, leads to the formation of small oligomers or scattered nanoparticles in our Brownian dynamics simulations as illustrated in Figs. 5(a) and 5(b) where the pair potential of Fig. 3(a) was used. In these simulations, linear nanoparticle chain arrays can occur as expected but are smaller than four to five monomer long mainly due to the very low probability of head-on collisions with the terminal nanoparticles in existing oligomers. Shown in Fig. 5(c) is our simulation result where a linear chain array grows by one monomer via a head-on collision with a dispersed nanoparticle that is beyond the potential cutoff initially and guided by an anisotropic potential energy surface similar to those delineated in Fig. 3. Substantially longer simulations with other systems such as two trimers or tetramer+dimer were also attempted but were unsuccessful in generating rare events of linear growth within the explored time frames due to the inherently low probabilities. Interestingly, the actual self-assembly processes are also fairly slow. The linear array of nanoparticles wiggles as they move as shown in Fig. 5(c), that is, the thermal disruptive effects are present. In all, neither closed packed structures appear to form nor do the linear oligomers develop into those when the full potentials are used.

A few features on the correspondence between the potential and the surfactant as inferred from the simulation studies are noted here. It has been stated earlier that  $r_{\text{outer}}$  is a separation where surfactant interdigitation starts and  $r_{\text{inner}}$  is

where surfactant interdigitation ends. ( $r_{\text{outer}} - r_{\text{inner}}$ ) in Eq. (5) spans a distance that is expected to be less than twice the fully extended length of the surfactant tail. The height of repulsion (measuring the difficulty of interdigitation) and sticking (measured by  $k_{\theta}$ ) are determined by the chain length and chain stiffness, and both of them need to have optimum values. Simulation studies using atomistic models can be undertaken in future to focus on these aspects.

The first few elements of the chain form “thermodynamically.” The effects of interdigitation that the model tries to reproduce in Eq. (5) appear to lead to “kinetic stabilization,” where both the effective anisotropic potential energy surface increases (Fig. 3) and sticking in Eq. (5) guide the nanoparticles to assemble in a linear array, but the latter continues to play a role as without it the particles in the linear array would eventually slide around each other to form a closed packed cluster. That is, it remains an important intra-floc force.

## CONCLUSIONS

Our work shows that together with the usual core repulsion and van der Waals attraction, a longer-range secondary repulsion and an angle-dependent sticking effect, both arising from surface-adsorbed surfactants, form a pair potential that is isotropic between individually dispersed surfactant-coated nanoparticles but result in anisotropic PES to promote the formation of chain arrays when the self-assembly starts. These two interaction components are also critically important in stabilizing assembled nanoparticle chain arrays. Brownian dynamics simulations show that there is no formation of chain arrays, that is, no self-assembly, if the parameters of the pair potential are altered to lie beyond a range, just as the self-assembly does not take place in the experiments outside a window of conditions. While finer-scale studies can be undertaken to further characterize the potential components and parameters considered in this work, the pair potential formulated here is believed to have a good value in simulating other larger-scale and more practical applications of self-assembly of surfactant-coated nanoparticles.

## ACKNOWLEDGMENT

This material is based on work supported by the National Science Foundation under Grant No. CTS-0113016.

- <sup>1</sup>W. P. Halperin, *Rev. Mod. Phys.* **58**, 533 (1986).
- <sup>2</sup>A. P. Alivisatos, *Science* **271**, 933 (1996).
- <sup>3</sup>Y. Volokitin, J. Sinzig, L. J. de Jongh, G. Schmid, M. N. Vargaftik, and I. I. Moiseev, *Nature (London)* **384**, 621 (1996).
- <sup>4</sup>J. D. Aiken III and R. G. Finke, *J. Mol. Catal. A: Chem.* **145**, 1 (1999).
- <sup>5</sup>A. N. Shipway, E. Katz, and I. Willner, *ChemPhysChem* **1**, 18 (2000).
- <sup>6</sup>H. S. Nalwa, *Handbook of Nanostructured Materials and Nanotechnology* (Academic, San Diego, 2000).
- <sup>7</sup>C. P. Collier, T. Vossmeier, and J. R. Heath, *Annu. Rev. Phys. Chem.* **49**, 371 (1998).
- <sup>8</sup>M.-C. Daniel and D. Astruc, *Chem. Rev. (Washington, D.C.)* **104**, 293 (2004).
- <sup>9</sup>G. M. Whitesides, J. P. Mathias, and C. T. Seto, *Science* **254**, 1312 (1991).
- <sup>10</sup>M. Brust and C. J. Kiely, *Colloids Surf., A* **202**, 175 (2002).
- <sup>11</sup>C. Gutiérrez-Wing, P. Santiago, J. A. Ascencio, A. Camacho, and M. José-Yacamán, *Appl. Phys. A: Mater. Sci. Process.* **71**, 237 (2000).
- <sup>12</sup>J. R. Heath, C. M. Knobler, and D. V. Leff, *J. Phys. Chem. B* **101**, 189 (1997).
- <sup>13</sup>R. A. Miron and K. A. Fichthorn, *Phys. Rev. B* **72**, 035415 (2005).
- <sup>14</sup>A. Ferral, P. Paredes-Olivera, V. A. Macagno, and E. M. Patrino, *Surf. Sci.* **525**, 85 (2003).
- <sup>15</sup>W. M. Gelbart, R. P. Sear, J. R. Heath, and S. Chaney, *Faraday Discuss.* **112**, 299 (1999).
- <sup>16</sup>Z. Zhang and S. Glotzer, *Nano Lett.* **4**, 1407 (2004).
- <sup>17</sup>T. K. Sau and C. J. Murphy, *Langmuir* **21**, 2923 (2005).
- <sup>18</sup>Z. Tang, N. A. Kotov, and M. Giermig, *Science* **297**, 237 (2002).
- <sup>19</sup>A. Y. Kim, K. D. Hauch, J. C. Berg, J. E. Martin, and R. A. Anderson, *J. Colloid Interface Sci.* **260**, 149 (2003).
- <sup>20</sup>C. Tien, C.-S. Wang, and D. T. Barot, *Science* **196**, 983 (1977).
- <sup>21</sup>T. C. Halsey, *Science* **258**, 761 (1992).
- <sup>22</sup>S. L. Biswal and A. P. Gast, *Phys. Rev. E* **68**, 021402 (2003).
- <sup>23</sup>J. N. Israelachvili, *Intermolecular and Surface Forces* (Academic, San Diego, 1991), pp. 176 and 288.
- <sup>24</sup>M. J. Vold, *J. Colloid Sci.* **16**, 1 (1961).
- <sup>25</sup>P. G. de Gennes, *Adv. Colloid Interface Sci.* **27**, 189 (1987).
- <sup>26</sup>Y. Qin and K. A. Fichthorn, *J. Chem. Phys.* **119**, 9745 (2003).
- <sup>27</sup>K. A. Fichthorn, M. L. Merrick, and M. Scheffler, *Phys. Rev. A* **68**, 041404(R) (2003).
- <sup>28</sup>J. E. Martin, J. P. Wilcoxon, J. Odinek, and P. Provencio, *J. Phys. Chem. B* **104**, 9475 (2000).
- <sup>29</sup>Z. L. Wang, S. A. Harfenist, R. L. Whetten, J. Bentley, and N. D. Evans, *J. Phys. Chem. B* **102**, 3068 (1998).
- <sup>30</sup>M. B. Einarson and J. C. Berg, *Langmuir* **8**, 2611 (1992).
- <sup>31</sup>J. Klein, E. Kumacheva, D. Mahalu, D. Perahia, and L. J. Fetters, *Nature (London)* **370**, 634 (1994).
- <sup>32</sup>J. Klein, *Colloids Surf., A* **86**, 63 (1994).
- <sup>33</sup>D. L. Ermak, *J. Chem. Phys.* **62**, 4189 (1975); D. L. Ermak and J. A. McCammon, *ibid.* **69**, 1352 (1978).
- <sup>34</sup>N. A. Frej and D. C. Prieve, *J. Chem. Phys.* **98**, 7552 (1993).
- <sup>35</sup>H. C. Öttinger, *Stochastic Processes in Polymeric Fluids* (Springer, Berlin, 1996).